Cinquina *et al. Clinical Proteomics* (2026) 23:20
https://doi.org/10.1186/s12014-026-09588-2

Clinical Proteomics

RESEARCH Open Access

Proximity extension assay-based serum proteomic profiling identifies shared protein signatures in hypermobile Ehlers–Danlos syndrome and hypermobility spectrum disorders

Valeria Cinquina[1], Giulia Carini[1], Nicola Chiarelli[1], Marika Vezzoli[1], Valeria Bertini[1], Marina Venturini[2], Woodrow Gandy[3], Marina Colombi[1] and Marco Ritelli[1*]

Abstract

Background Hypermobile Ehlers-Danlos syndrome (hEDS) and hypermobility spectrum disorders (HSD) are prevalent conditions characterized by symptomatic joint hypermobility and a substantial public health burden, for which no causal treatment is currently available. In the absence of a defined molecular basis or validated diagnostic biomarkers, diagnosis of hEDS relies solely on the 2017 clinical criteria, with individuals who do not meet these criteria classified as HSD. Although currently categorized as distinct entities, the biological relationship between hEDS and HSD remains a subject of active debate within the scientific community.

Methods We performed targeted serum proteomic profiling using the proximity extension assay technology, quantifying 458 proteins in large cohorts of hEDS ($n=88$) and HSD ($n=88$) patients, alongside healthy controls ($n=176$).

Results Compared to controls, 54 proteins were differentially expressed in hEDS patients and 49 in HSD patients. No statistically significant differences were observed between hEDS and HSD groups. When the combined patient cohort was analyzed, 69 proteins showed differential expression relative to controls. The proteins were distributed across the predefined PEA panels, which include proteins involved in inflammatory, cardiometabolic, neurological, organ damage, and developmental processes.

Conclusions This targeted serum proteomic analysis identified overlapping protein expression changes in hEDS and HSD relative to controls, while revealing no detectable differences between the two conditions. These findings suggest the presence of shared molecular features across the hEDS/HSD spectrum and identify a set of candidate circulating proteins that warrant further investigation and independent validation in larger, well-characterized cohorts.

*Correspondence:
Marco Ritelli
marco.ritelli@unibs.it

Full list of author information is available at the end of the article

Keywords Hypermobile Ehlers-Danlos syndrome, Hypermobility spectrum disorders, Serum, Proteomics, Proximity extension assay

Introduction

Hypermobile Ehlers-Danlos syndrome (hEDS) is a multisystemic heritable connective tissue disorder (HCTD) characterized by generalized joint hypermobility (JHM), musculoskeletal complaints, and a wide array of comorbidities that significantly impair patients' quality of life [1–3]. Due to the absence of an identified molecular basis or validated laboratory tests, the diagnosis of hEDS relies exclusively on clinical criteria established in 2017 [2]. Individuals presenting with symptomatic JHM who do not fulfill these criteria, and who do not meet diagnostic requirements for other JHM–associated conditions, are currently classified as having hypermobility spectrum disorders (HSD). Despite sharing similar symptoms and functional complications with hEDS, including numerous extra-articular manifestations not captured by current diagnostic criteria, these conditions remain formally distinct [3–7].

Consequently, there is ongoing debate within the scientific community regarding whether hEDS and HSD represent biologically distinct disorders or instead reflect a phenotypic continuum within a shared disease spectrum [4, 7–11]. This diagnostic uncertainty not only places a substantial burden on healthcare practitioners but also significantly impacts patients, with wide-ranging consequences for a significant portion of the global population. Indeed, epidemiological evidence from large population-based datasets, including medical records from Wales, suggest that the combined prevalence of hEDS and HSD is likely greater than 1 in 500 individuals [7, 12, 13].

In clinical practice, diagnosing, classifying, and managing hEDS and HSD patients remains extremely challenging. In the absence of clear molecular markers and amid ongoing nosological debate, patients frequently face prolonged diagnostic pathways characterized by uncertainty and vulnerability, particularly individuals with HSD in countries where this condition is not formally recognized within public healthcare systems. Diagnostic delay is substantial, with recent survey-based studies reporting mean delays ranging from approximately 10 to over 20 years from symptom onset to diagnosis, often accompanied by misdiagnoses and inappropriate treatments [14, 15]. Limited awareness among healthcare professionals further contributes to patient dismissal or stigmatization with symptoms frequently misattributed to psychosomatic or psychiatric causes [14–18].

Although awareness of these conditions is increasing, particularly among clinical geneticists, many primary care providers remain skeptical or poorly informed [19]. This skepticism perpetuates patients' suffering as they struggle to find practitioners who acknowledge and address their debilitating, multisystemic symptoms, which extend far beyond joint instability. These include chronic pain and fatigue, functional gastrointestinal disorders, cardiovascular dysautonomia, gynecological and bladder concerns, neurological symptoms, psychological and psychiatric issues, temporomandibular joint dysfunction, various orthopedic problems, and immune system alterations [5, 20].

Within this complex clinical scenario, further complicated by limited understanding of disease mechanisms and the lack of effective targeted therapies, our research group has gathered a body of experimental evidence supporting the presence of shared pathophysiological features in hEDS and HSD [7–9, 11, 21]. In a series of studies, we reported widespread extracellular matrix (ECM) disorganization and altered inflammatory signaling in dermal fibroblasts derived from both hEDS and HSD patients, accompanied by increased protease activity and the production of ECM-derived degradation fragments. Consistently, specific fibronectin and type I collagen fragments were recently detected in plasma samples from individuals with hEDS and HSD, whereas these fragments were absent in healthy individuals. While these findings suggest that ECM-related molecular alterations identified in vitro may be reflected in circulation, independent validation of these candidate markers is lacking, and systematic characterization of the circulating proteins in hEDS and HSD are scarce. Recent work by Griggs et al. [22] applied unbiased mass spectrometry–based proteomics to a discovery cohort of 29 women with hEDS, identifying immune-related protein alterations, particularly within the complement cascade, consistent with an earlier study by Watanabe et al. [23]. The study by Griggs et al. was further strengthened by orthogonal validation via ELISA in an expanded cohort that included male participants. These findings challenge the traditional view of hEDS as solely a connective tissue disorder and support a revised paradigm that includes innate immune dysfunction, providing novel insights into disease pathophysiology. However, despite these advancements, comparative proteomic analyses directly encompassing and comparing both hEDS and HSD populations are still missing.

In this context, the present study aimed to characterize serum protein expression patterns in both hEDS and HSD using a targeted proteomic approach. We analyzed serum samples from large cohorts of hEDS and HSD patients and healthy individuals using proximity extension assay (PEA) technology, which enables sensitive

and specific quantification of predefined protein panels from minimal sample volumes [24]. By profiling 458 circulating proteins across multiple biological domains, this study seeks to identify shared and condition-specific serum protein alterations in hEDS and HSD and to provide a foundation for future hypothesis-driven validation studies.

Methods

Study approval

The study was approved by the local Ethical Committee "Comitato Etico di Brescia, ASST degli Spedali Civili, Brescia" in Italy (Protocol Number NP5582) and by the "Genetic Alliance Institutional Review Board" in the USA (Federal Registration Number IORG0003358, Project number EDS002). The study was conducted according to the principles of the Declaration of Helsinki and the Good Clinical Practice (GXP) guidelines. Prior to participation, written informed consent was obtained from all individuals.

Study design and participants

This study involved a total of 352 participants (aged ≥ 18 years), including individuals with hEDS and HSD, healthy controls, enrolled through two distinct institutions. The Italian cohort was recruited at the specialized outpatient clinic for Heritable Connective Tissue Disorders and EDS at the University Hospital Spedali Civili of Brescia and consisted of 44 hEDS (40 females and 4 males, P1-P44), 44 HSD patients (34 females and 10 males, H1-H44), and 176 healthy donors (C1-C176). An independent American cohort, provided by the Ehlers-Danlos Society (New York, NY, USA) included 44 hEDS (42 females and 2 males, P45-P88) and 44 HSD (all females, H45-H88) patients.

Regarding the Italian cohorts, the diagnosis of hEDS (or HSD) relied on direct clinical assessment according to the 2017 hEDS criteria [2, 7] with the widely endorsed modification of considering gJHM (criterion 1) as positive for patients scoring one-point below the age-specific Beighton Score (BS) cutoff [3, 7] in the presence of a positive 5-point questionnaire (5PQ) [25]. Symptomatic patients, with at least one musculoskeletal manifestation who did fulfill these adjusted hEDS criteria were classified as HSD [7].

As part of the HEDGE project, all American patients were registered into the "DICE EDS and HSD Global Registry" and completed a REDCap survey that collected detailed clinical data. The inclusion criteria for the American hEDS group were the 5PQ-adjusted 2017 hEDS criteria, determined by (i) direct exam and interview or (ii) review of medical records through the EDS and HSD registry and sometimes photographs of certain features amenable to photographic confirmation. The inclusion criteria for the American HSD patients comprised a 2018 or later diagnosis based on the absence of eligibility for the 2017 hEDS criteria. Specifically, patients were selected for positivity for criterion 1, fewer than 5 feature 2 A findings, and presence of at least one musculoskeletal manifestation (Feature C) based solely on survey data, without further medical record investigation or physical examination.

In both the Italian and American patient cohorts, a range of comorbid conditions were recorded through direct clinical assessment and interviews, and patient-provided medical reports review, or self-reporting in the REDCap survey. These comorbidities were defined as follows: (i) functional gastrointestinal disorders: gastroesophageal reflux, gastroparesis, dysmotility, constipation, diarrhea, irritable bowel syndrome, abdominal pain; (ii) neurological issues: headaches/migraines, neuropathic pain, allodynia, paresthesia, peripheral neuropathy, dizziness, "brain fog", difficulty with memory and concentration; (iii) cardiovascular dysautonomia: abnormal heart rate responses, irregular heart rhythms, orthostatic intolerance, exercise intolerance, postural orthostatic tachycardia syndrome (POTS) confirmed by tilt table testing, (iv) psychological/psychiatric issues: depression, anxiety disorders, sleep and mood disorders, obsessive-compulsive disorder, attention-deficit/hyperactivity disorder; (v) bladder/urological issues: urinary incontinence, overactive bladder, neurogenic bladder, urinary retention, pelvic organ prolapse; (vi) gynecological concerns: meno/metrorrhagia, disabling dysmenorrhea, pelvic pain, dyspareunia, and vulvodynia; vi) chronic fatigue: persistent, unexplained, and severe fatigue lasting for at least 6 months and not relieved by rest or sleep; (vii) temporomandibular joint disorders: of the jaw muscles, temporomandibular joints, and the nerves associated with chronic facial pain; vii) allergic/atopic issues: food/drug/insect allergies, asthma, atopic dermatitis, rhinitis/rhinoconjunctivitis, mast cell activation syndrome (MCAS) confirmed by an immunologist.

For the control group, which comprised 160 females and 16 males, individuals had to meet the following criteria: they had to be unrelated to anyone with hEDS or HSD and must not exhibit any signs or symptoms of these conditions upon physical examination and interview.

Storage and handling of serum samples

Serum samples from Italian participants were collected, processed, and stored according to the following protocol: 3.5 ml of whole blood was collected in BD Vacutainer® serum separator tubes, centrifuged at 2,500 g for 15 min at room temperature within one hour of collection, the supernatant divided into aliquots, and stored at −80 °C until analysis.

Blood samples from American participants were collected at their homes following standard operating procedures to minimize pre-analytical variation. Trained phlebotomists drew 3.5 ml of peripheral blood into BD Vacutainer® serum separator tubes, and samples were stored at 4 °C during transport to the processing laboratory in Baltimore within 24 h of collection. Upon arrival, samples were centrifuged at 2,500 g for 15 min at room temperature, then aliquots of the supernatant were transferred to cryovials and frozen at −80 °C. Frozen aliquots were then shipped on dry ice to the Italian facility for centralized handling. To minimize potential bias and mitigate batch effects arising from different collection sites and processing timelines, all samples were randomized across four 96-well plates using a dedicated R script provided by Olink. This randomization ensured a balanced distribution of hEDS, HSD, and control samples, as well as an even distribution of Italian and American cohorts across all plates. The randomized plates were shipped on dry ice to the Olink Proteomics laboratory (Uppsala, Sweden), where protein quantification was performed as a fee-for-service.

Proximity extension assay

Proteomic measurements were performed using five manufacturer-validated Olink® Target 96 panels: Neurology (v.8013), Organ Damage (v.3311), Development (v.3521), Cardiometabolic (v.3604), and Inflammation (v.3024), for a total of 460 assays (Additional Table 1). The Olink PEA is a high-throughput, multiplexed proteomic platform that utilizes a dual-recognition mechanism to ensure high specificity. For each protein target, a pair of oligonucleotide-labeled antibodies (PEA probes) must bind in close proximity, allowing their respective DNA oligos to hybridize. This hybridization event is followed by DNA polymerase-mediated extension and subsequent quantification via real-time quantitative PCR. Proteins were provided as normalized protein expression (NPX) values, which are arbitrary units on a $\log_2$ scale representing relative quantification (Additional Table 2).

Quality control and normalization

Initial quality control (QC) and normalization were performed by Olink, with all measurements performed blinded to clinical status. Intensity Normalization (v.2) was applied across all five panels to ensure data comparability across the four plates used. Olink's internal QC process utilizes four internal controls added to every sample to monitor assay performance and individual sample quality: two incubation controls (non-human antigens), one extension control (an antibody linked to two matching oligonucleotides), and one detection control (a double-stranded DNA piece). These controls monitor all steps of the assay from antibody binding to qPCR. The QC was conducted in two distinct steps: i) Plate-level QC, where each sample plate was evaluated based on the standard deviation of internal controls, with a required threshold of <0.2 NPX; and ii) Sample-level QC, where individual sample quality was assessed by calculating the deviation from the median value of the internal controls. Samples deviating by less than 0.3 NPX passed the quality control. Out of 352 serum samples, 344 to 351 samples passed QC depending on the specific panel. Data points for samples failing these criteria were flagged with a 'QC Warning'; samples with severe deviations were set to 'No Data' in the final output file to ensure data integrity. The technical reliability was confirmed by the Coefficient of Variance (%CV), calculated from pooled control samples. The average intra-assay %CV was $\leq 8\%$ across all panels, while the average inter-assay %CV was $\leq 20\%$, demonstrating high reproducibility. Furthermore, protein detectability (percent of proteins > LOD) was high, ranging from 85% (Inflammation) to 98% (Neurology). Detailed QC results are provided in Appendix 1.

Statistical analysis

Descriptive statistics were computed for all the proteins, including number of missing values (N-Miss), mean, standard deviation (SD), median, first (Q1) and third (Q3) quartile, and range. Prior to differential expression (DE) analysis, duplicated proteins (e.g., GDNF and Beta-NGF) were removed by retaining values from only one panel, resulting in 458 unique protein assays. Furthermore, individual NPX values flagged with 'QC Warning' were excluded (Additional Table 2). Proteins with NPX values below the limit of detection (LOD) in more than 30% of samples in both the patient and control groups were also removed. For the remaining 424 proteins (Additional Table 3), NPX values below the LOD were replaced with the LOD value, consistent with Olink's recommendations for statistical analysis.

Comparisons between protein levels of affected individuals (hEDS or HSD) versus healthy controls (Affected vs. Control) were computed using the Wilcoxon Rank Sum test, which is well suited when variables analyzed are not normally distributed; indeed, Shapiro test p-values were calculated for all the proteins in the dataset and were found to be <0.05. The Benjamini-Hochberg (BH) correction was used to control the false discovery rate (FDR) during multiple hypothesis testing. This bivariate analysis selected a limited number of proteins significantly different between the two groups (Affected vs. Control).

To enhance the interpretability and predictive accuracy of our analysis, the Least Absolute Shrinkage and Selection Operator (LASSO) was applied, a penalized regression technique that performs both variable selection and regularization [26]. In this context, the dependent

variable was the diagnosis (Affected versus Control), whereas the set of predictors consisted of the proteins found to be differentially expressed by the Wilcoxon Rank Sum test. LASSO addresses limitations of classical linear regression, by penalizing the absolute size of the regression coefficients and driving some of them to zero, thereby excluding non-influential predictors. This process is controlled by a tuning parameter (λ), which defines the strength of the penalty: as λ increases, more coefficients are set to zero, leading to a more interpretable model. The optimal value of λ was automatically chosen by means of the cross-validation procedure that fits a model for each λ selecting that value that generates the smallest Mean Squared Error (MSE).

To conduct LASSO estimation missing values were addressed using the MissForest algorithm [27], which considers complex interactions and nonlinear relationships between outcome and covariates and is robust to noisy data and multicollinearity. Because LASSO considers the predictive power of variables collectively, accounting for correlations among covariates, it may lead to different results than the bivariate Wilcoxon Rank Sum test.

To further investigate the relationship between the outcome (Affected vs. Control) and the covariates selected by LASSO from the 69 proteins identified through the Wilcoxon rank-sum test, an ensemble model belonging to the family of machine learning methods, namely the Random Forest (RF) [28–30], was estimated from which two additional informative tools were obtained. The first one is the relative Variable Importance Measure (relVIM) [31–33], which identifies the covariates that have the strongest impact in classifying subjects. It provides a ranking from the most (relVIM = 100, at the bottom of the graph) to the less important variable visualizing it by means of a lollipop plot where in x-axis are reported the relVIM values and in y-axis the covariates [34]. The second one is the 3D Partial Dependence Plot (PDP) [35] that visualizes how the probability of being classified as "Affected" changes with the variation of the three most important protein values identified by the relVIM. For a conclusive visualization of the acquired results, a single classification tree was constructed. This approach identifies homogeneous patient clusters with respect to the model's outcome (Affected vs. Control), based on the same set of covariates (namely, the proteins selected by LASSO) previously used in the Random Forest [30].

For completeness, the RF along with the computation of the relative relVIM, the 3D-PDP, and classification tree analyses were repeated using the full set of 69 proteins by the Wilcoxon rank-sum test. This additional step aimed to assess how the selection of covariates through LASSO influenced the results, by comparing them to those obtained when the analysis was conducted directly on the broader set of candidate proteins.

All analyses were run in R, version 4.5.1 and the following R packages were used: readxl, arsenal, MASS, ggplot2, missForest, glmnet, randomForest, pdp, rpart, rpart.plot.

Functional enrichment analysis

Functional enrichment analysis of DEPs was performed by querying STRING database. We also explored enriched Gene Ontology (GO) biological processes by Enrichr online tool, and Kyoto Encyclopedia of Genes and Genomes (KEGG) pathways based on an FDR-corrected p-value threshold ≤ 0.05. To characterize the functional role of the most clinically relevant candidate proteins, the Cytoscape app ClueGO was used to query GO (Biological Process), KEGG, Reactome, and WikiPathways. A two-sided hypergeometric test (BH-corrected) determined the probability of functional terms being assigned to the gene sets.

All analyses and data visualization were conducted in R, version 4.5.1 unless otherwise stated. The following R Bioconductor packages were used for data visualization: ClusterProfiler version 4.10 provides functions, such as enrichGO and enrichKEGG, for conducting enrichment tests on GO terms and KEGG pathways. These tests are based on the hypergeometric distribution. Moreover, the package supports the visualization of enrichment results using ggplot2 version 3.5.1, an open-source data visualization package that has been employed for creating volcano plots, pie charts, and bar charts [36].

Results

Clinical characteristics and diagnostic classification

This study includes a total of 352 participants, 88 individuals clinically diagnosed with hEDS (P1-P88, 82 females and 6 males, with a mean age of 36 years, standard deviation [SD] 11.7, range 18–71), 88 with HSD (H1-H88, 78 females and 10 males, with a mean age of 38 years, SD 11.6, range 18–65), and 176 Italian healthy individuals (160 females and 16 males, mean age 42 years, SD 14.2, range 20–68). Patients were selected from two distinct cohorts: one Italian (P1-P44 and H1-H44) and the other American (P45-P88 and H45-H88). All patients were classified according to the diagnostic criteria defined in the 2017 EDS nosology. Comprehensive clinical details for each enrolled patient can be found in Additional Table 4. The overall frequencies of the three required diagnostic criteria for diagnosing hEDS across both cohorts are summarized in Fig. 1A, while the distribution of assessed comorbid conditions is presented in Fig. 1B. Further clinical detail, including subgroup-specific frequencies and criteria fulfillment, is provided in Additional Fig. 1 A and Additional Table 5, and 6. A detailed

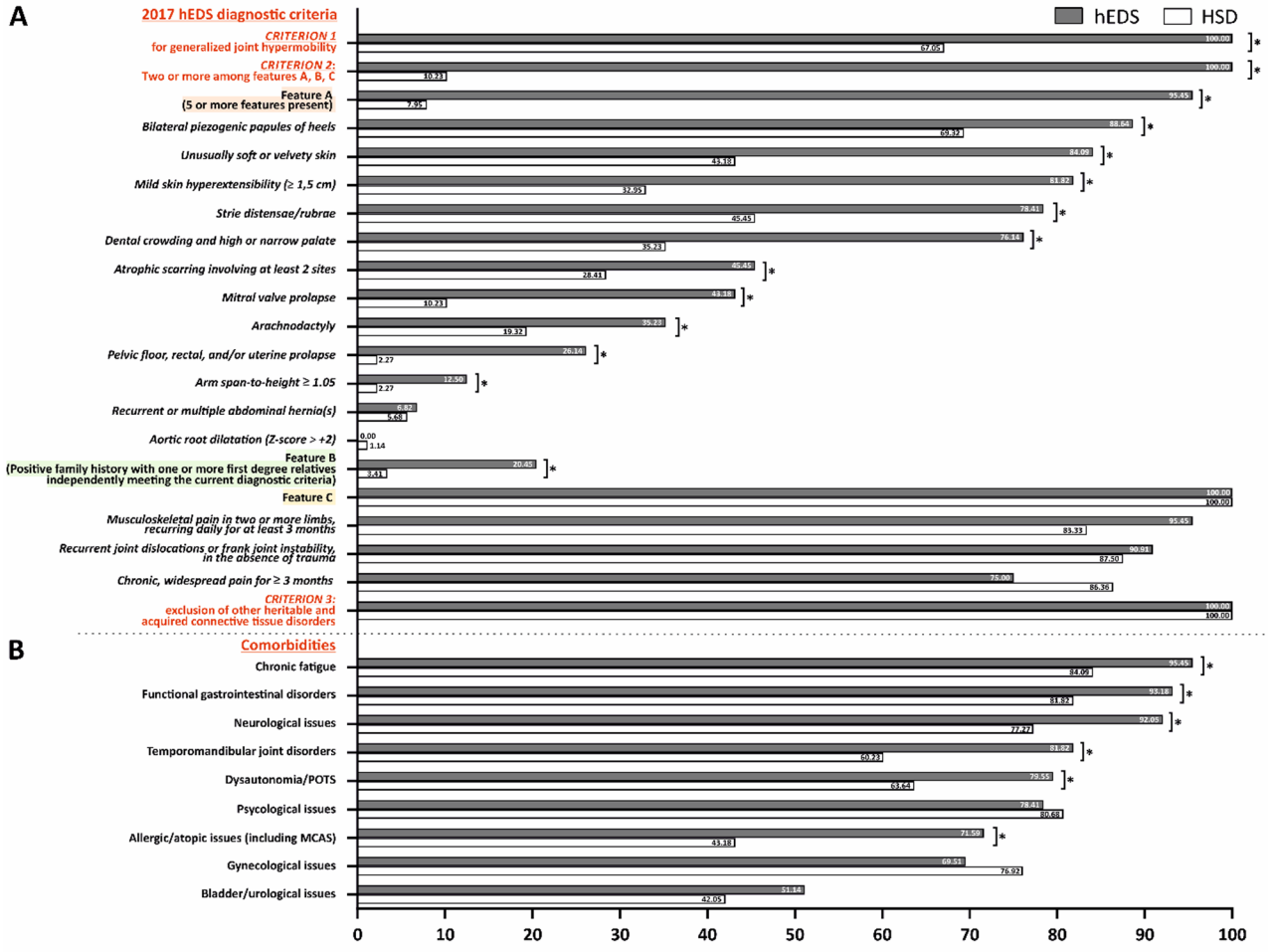

Fig. 1 A summary of three required diagnostic criteria for an hEDS diagnosis in the entire cohort of 176 patients: 88 with hEDS and 88 with HSD in accordance with the 2017 EDS classification (**A**). The overall distribution of assessed comorbid conditions in the full cohort population (**B**). *Presence of statistically significant differences between hEDS and HSD individuals

description of the familial structure and specific phenotypic comparisons between geographical subgroups is provided in Supplementary File 1.

PEA-based serum proteomics reveals a shared systemic dysregulation of Circulating proteins in hEDS and HSD patients

To identify any protein expression signatures and associated disease pathways that were shared or unique between the two cohorts of patients with hEDS and HSD, a PEA-based proteomic screening was performed comparing serum samples from 88 hEDS patients (44 Italian and 44 American), 88 HSD patients (44 Italian and 44 American), and 176 Italian healthy volunteers as a control group (Fig. 2A) This multi-panel targeted analysis included the examination of a total of 458 unique proteins involved in several key biological processes such as inflammatory and immune responses, regulation of cell migration, motility, proliferation, cell cycle, cell death/apoptosis, extracellular matrix organization, neurogenesis, response to stress, and cardiovascular, cardiometabolic, and neurological functions (Additional Table 1). After quality control and data cleaning (Appendix 1), 424 proteins were filtered for further statistical and biological analyses (Additional Table 2).

In the initial stage of our screening, we conducted separate comparisons to analyze the differential expression of proteins among three groups: 88 individuals with hEDS compared to 176 controls, 88 individuals with HSD compared to 176 controls, and 88 individuals with hEDS compared to 88 individuals with HSD (Additional Table 7). As shown in Fig. 2A and Additional Fig. 3A. A total of 54 DEPs, comprising 19 downregulated and 35 upregulated, were identified in hEDS patients compared to controls. Likewise, for HSD, a volcano plot analysis unveiled 49 proteins that met filtering criteria, showing 3 downregulated and 46 upregulated proteins across the cohorts (Fig. 2A, Additional Fig. 3B). The distribution of these identified DEPs across their respective Olink proteomic panels was visually represented through a pie chart to

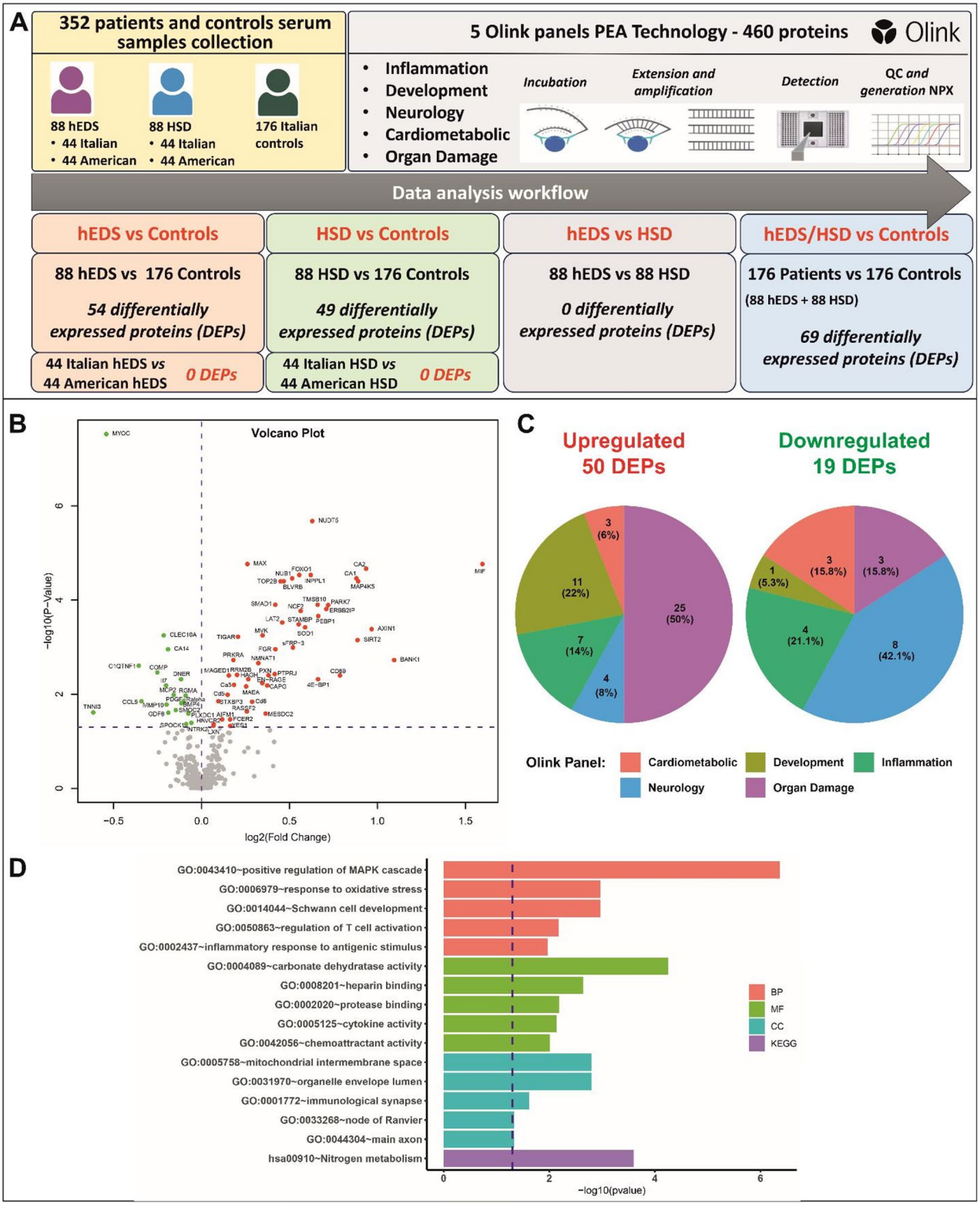

Fig. 2 (See legend on next page.)

(See figure on previous page.)

Fig. 2 Exploring serum protein dysregulation in a cohort of 176 hEDS/HSD patients compared to healthy individuals. Study design and data analysis workflow involving comparisons of hEDS vs. controls, HSD vs. controls, and hEDS/HSD vs. controls across both Italian and American cohorts (**A**). A volcano plot displays the 69 DEPs (50 up- and 19 downregulated) identified in serum samples from patients with hEDS and HSD (**B**). A pie chart graph visually represents the distribution of the 50 up- and 19 downregulated proteins across the analyzed Olink protein marker panels; note that these categories reflect the assay's panel architecture rather than exclusive biological specificity (**C**). Functional enrichment analysis has been performed using the Enrichr online tool, considering GO terms related to biological process (BP), molecular function (MF), cellular component (CC), as well as the Kyoto Encyclopedia of Genes and Genomes (KEGG) pathway (**D**). GO terms for each category are plotted according to the -log10 p-value. Additionally, we performed a STRING protein-protein interaction network analysis on the 69 DEPs

illustrate the technical breadth of the screening. Notably, there were no DEPs identified upon comparison of the 88 samples of hEDS with the 88 samples of HSD (Fig. 2A, Additional Table 7). This observation aligns with our earlier RNA-seq findings [11], further reinforcing the idea that hEDS and HSD share common protein signatures and a disease-associated profile that extends beyond variations in gene expression [11].

Moreover, we investigated potential variations in protein expression between the Italian and American patient groups. Remarkably, our comparative examination revealed the absence of DEPs when comparing the 44 Italian individuals with hEDS and their American counterparts. Similarly, no DEPs were observed when comparing 44 individuals with HSD from Italy to those from the United States (Fig. 2A, Additional Table 7).

In light of these findings, we performed an additional analysis, considering hEDS and HSD as a single clinical entity. The Italian and American patients affected by either condition were grouped together under the label hEDS/HSD and compared to the control samples. The volcano plot showed a total of 69 statistically significant DEPs (FDR-adjusted p-value < 0.05) in patient group, consisting of 19 downregulated and 50 upregulated proteins (Fig. 2B, Additional Table 7). Notably, these DEPs were distributed across their respective Olink proteomic panels, including those related to cardiometabolic, inflammation, neurology, development, and organ damage (Fig. 2C), suggesting a systemic dysregulation of protein abundance in patient serum samples.

To explore the biological consequences of these protein changes, the 69 DEPs were subject to GO functional enrichment analyses (Fig. 2D). The most representative KEGG biological processes including positive regulation of MAPK cascade, response to oxidative stress, Schwann cell development, regulation of T cell activation, and inflammatory response to antigenic stimulus, emerged as the most significantly affected biological functions. The most perturbed molecular functions included carbonate dehydratase activity, heparin binding, protease binding, cytokine activity, chemoattractant activity, whereas mitochondrial intermediate space, organelle envelope lumen, immunological synapse, node of Ranvier, and axon were the most enriched cellular component GO terms. KEGG pathways analysis revealed an enrichment of nitrogen metabolism. A complete list of all enriched GO terms is available in Additional Table 8.

Functional enrichment of the 50 upregulated proteins revealed several clusters comprising proteins associated with the one-carbon metabolic process (CA1, CA2, and CA3), cellular response to oxidative stress (ERBIN, PXN, SOD1, INPPL1, EIF4EBP1, FOXO1, SIRT2, AXIN1, MIF), regulation of neural death (TIGAR, NMNAT1, PARK7), regulation of defense, inflammatory response, and lymphocyte activation (NCF2, S100A12, FGR, YES1, PARK7, MIF, CD5, CD6, SOD1), as well as regulation of innate immune response/system (S100A12, FGR, YES1, NCF2, FCER2, CD5, CD6, PTPRJ, MIF) (Fig. 3A). The most enriched clusters of the 19 downregulated proteins comprised various functions associated with immunity and inflammation, such as eosinophil and macrophage chemotaxis (CCL5, CCL8, MSTN), regulation of leukocyte proliferation (IL7, BMP4, CCL5, CCL8), blood vessel morphogenesis (PDGFRA, NTRK2, SMOC2), ECM organization (MMP10, PDGFRA, SMOC2), and intracellular signaling via protein kinases (Fig. 3B).

We also created functionally organized networks to gain a deeper understanding of the biological terms and functional pathways associated with protein changes (Fig. 3C). Most of these biological networks were enriched by upregulated DEPs (Additional Table 9). Consistent with our prior transcriptome and proteome investigations [8, 9, 11, 37], the predominant upregulated biological networks were implicated in metabolic processes, intracellular homeostasis, inflammatory and immune response. These included functional hubs such as "lactate metabolic process", "hexokinase activity", "reversible hydration of carbon dioxide", "regulation of inflammatory response to antigenic stimuli", "immune response-regulating cell surface receptor signaling pathway involved in phagocytosis", "negative regulation of defense response to bacterium", "gene and protein expression by JAK-STAT signaling after Interleukin-12 stimulation", and "negative regulation of myeloid cell apoptotic process". Conversely, downregulated DEPs were enriched in functional clusters primarily associated with the regulation of macrophage chemotaxis, encompassing processes such as negative regulation of lymphocyte apoptotic process and phospholipase activator activity, such as eosinophil chemotaxis.

Machine Learning-based predictive modeling

By computing the descriptive statistics on all proteins and stratifying by diagnosis (Affected vs. Control), the Wilcoxon Rank Sum test, adjusted with the BH method, identified 69 of the 424 proteins as significantly differentially expressed between the two groups (Additional Table 7).

To assess the relative contribution of these 69 DEPs, a RF model was initially constructed using these proteins as covariates and the diagnostic classification (hEDS or HSD vs. Control) as the outcome. An ensemble of 10,000 classification trees were grown, with the algorithm randomly selecting a subset of covariates ($q = \sqrt{\#covariates} = \sqrt{69}$) at each node split. This approach generates a collection of weakly correlated models, each with limited individual predictive power. However, when aggregated, their collective output results in a robust and accurate classifier, namely a phenomenon commonly referred to as the "wisdom of crowds," wherein individual errors are mitigated through averaging across multiple decision trees.

The relative Variable Importance Measure (relVIM) was extracted from this model to identify the most influential proteins for classification within the set of 69 candidates. The variables were ranked by importance, with MYOC, NUDT5, and CLEC10A emerging as the top three contributors (Additional Table 10). They were used to generate a 3D-PDP; (Fig. 4A), illustrating how the probability of being classified as "Affected" varies with expression levels. Specifically, the probability reaches 0.60 when MYOC levels are low and CLEC10A levels are high. In this context, NUDT5 appears less informative, as the probability of being classified as affected increases both at median and high expression levels, resulting in a relatively flat response surface (Fig. 4A).

Using the same outcome (hEDS or HSD vs. Control) and the 69 proteins as covariates, a single classification tree was also constructed (Fig. 4B). This approach is useful for elucidating the complex interactions among proteins and their influence on the diagnostic outcome. By identifying threshold values along the protein expression continuum, the tree partitions subjects into homogeneous clusters (final nodes), each characterized by a distinct probability of being classified as Affected or Control. Notably, the primary splits involve MYOC, BLVRB, and MAX, reinforcing their prominent discriminative role.

Focusing on nodes labeled as "Affected":

- NODE 3: for high values of MYOC (≥ 3.9), low values of BLVRB (< 0.67), high values of FCER2 (≥ 6.10) and low values of MCP2 (< 8.90), the probability of being Affected is 67%.
- NODE 4: for high values of MYOC (≥ 3.9) and high values of BLVRB (≥ 0.67), the probability of being Affected is 69%.
- NODE 6: for low values of MYOC (< 3.90), low value of MAX (< 0.07) and high values of MESDC2 (≥ 2.20), the probability of being Affected reaches the value of 67%.
- NODE 7: for low values of MYOC (< 3.90) and high values of MAX (= 0.07), the probability of being Affected reaches the value of 78%.

To further refine the feature set, missing values were imputed using the missForest algorithm, and LASSO regression was applied to the 69 DEPs. The optimal value of the regularization parameter (λ = 0.0200) was identified through cross-validation (Additional Fig. 4), yielding a penalized regression model that retained 17 highly relevant predictors (Additional Table 11). These 17 proteins were subsequently used as covariates in a second RF model with the same outcome. To ensure methodological consistency, the same parameter settings were applied as in the previous analysis: 10,000 classification trees were grown, and at each node split, a random subset of covariates ($q = \sqrt{\#covariates} = \sqrt{17}$), was selected.

From this second RF, relVIM values were again extracted (Additional Table 12), with MYOC, TOP2B, and INPPL1 identified again as the most informative features. These three proteins were used in a new 3D-PDP (Fig. 4C), showing that the probability of being classified as "Affected" reaches 0.70 when MYOC is low and both TOP2B and INPPL1 are high.

A second classification tree was generated using the 17 proteins selected by LASSO as covariates and the diagnostic status (hEDS or HSD vs. Control) as the outcome (Fig. 4D). Once again, MYOC was the first split, followed by MAP4K5 and MIF at the second level, reinforcing their importance.

Looking at Fig. 4D and focusing again on nodes labeled as "Affected":

- **NODE 3**: for high values of MYOC (≥ 3.9), MAP4K5 (≥ 4.40), SMOC2 (≥ 7.50) jointly with low values of MCP2 (< 8.90), the probability of being affected is 61%.
- **NODE 4**: for high values of MYOC (c 3.9), MAP4K5 (≥ 4.40), jointly with low values of SMOC2 (< 7.50), the probability of being affected is very high, namely 92%.
- **NODE 7**: for low values of MYOC (< 3.9), high values of MIF (≥ 3.20), low values of TOP2B (< 3.20) and high values of HAVCR2 (≥ 1.60), the probability of being affected is 72%.

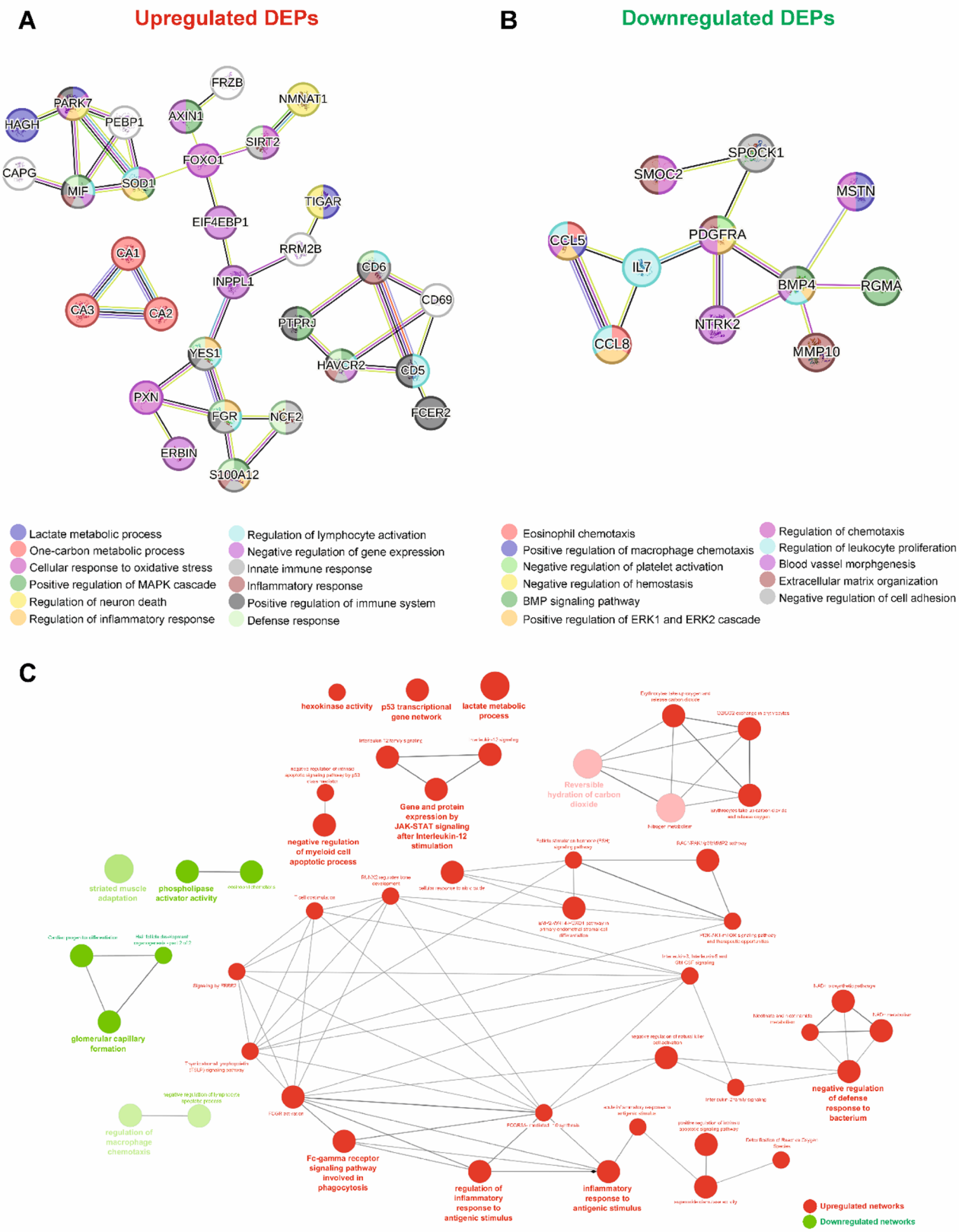

Fig. 3 (See legend on next page.)

(See figure on previous page.)

Fig. 3 High-confidence protein–protein interactions and biological network enrichment of 69 DEPs. STRING functional protein interaction networks of up- (**A**) and downregulated (**B**) proteins. Each node represents a protein, and each edge represents an interaction including either physical or functional associations. Enriched biological networks based on the up- and downregulated DEPs identified in hEDS/HSD serum samples, integrating GO-Biological Process with WikiPathways, KEGG, and Reactome databases, using the ClueGO plugin in Cytoscape. Terms (as nodes) are linked based on their κ score level (0.7), which defines term-term interactions (edges) and functional groups based on shared genes between the terms. Only enriched terms with Bonferroni step down-adjusted p-value ≤ 0.01 were considered

- **NODE 8**: for low values of MYOC (< 3.9), high values of MIF (≥ 3.20) and TOP2B (≥ 3.20), the probability of being affected is 80%.

Altogether, this multi-step approach, transitioning from the 69-DEP discovery set to a refined 17-protein LASSO selection, provides consistent and robust evidence for a specific proteomic signature that distinguishes hEDS/HSD patients from healthy individuals.

Discussion

Due to their multisystemic and clinically heterogeneous nature, hEDS and HSD pose challenges that persist despite decades of research, primarily due to the lack of a known molecular basis, consistent laboratory tests, and reliable biomarkers. This study represents the first large-scale investigation to utilize a targeted, multi-panel proteomic approach across international cohorts of both hEDS and HSD patients. Our goal was to identify a specific set of blood proteins distinguishing patients from healthy individuals, potentially serving as candidate protein signature to enhance clinical management and guide future therapeutic investigations. Employing a targeted high-throughput proteomic approach, we examined serum levels of 458 circulating proteins across panels dedicated to inflammation, cardiometabolic activity, neurological function, organ impairment, and developmental processes. Initially, we compared American and Italian hEDS and HSD patients separately with healthy donors and directly compared hEDS to HSD patients. Notably, we found no statistically significant protein differences when comparing hEDS patients between Italy and the USA, nor when comparing HSD patients across these distinct geographies. Most importantly, direct comparisons between the hEDS and HSD cohorts revealed no significant differential protein expression. To further validate the stability of this signal, we conducted independent analyses comparing each diagnostic group against the healthy control baseline. These separate screenings yielded a remarkably consistent set of 54 DEPs for hEDS and 49 DEPs for HSD, with a vast majority of proteins being shared between the two lists.

While we acknowledge that the absence of statistically significant divergence does not definitively imply molecular equivalence, as it may be influenced by factors such as cohort heterogeneity, limited statistical power, or assay sensitivity, it provided a pragmatic rationale for analyzing the combined cohorts as a unified group (hEDS/HSD). The identification of a shared dysregulated protein expression pattern, observed consistently in both groups prior to cohort merging, points toward a substantial molecular overlap in our dataset rather than distinct condition-specific signatures. While hEDS and HSD may present with varying clinical phenotypes, these findings are compatible with a common systemic signature, aligning with growing biological data questioning the clear-cut separation of these disorders at the molecular level [8, 10, 11, 21]. Such potential biological overlap suggests that current diagnostic boundaries might not fully capture the shared underlying pathophysiology, supporting the ongoing discussion within the expert community regarding the need to refine classification systems [7]. We further acknowledge that these findings are based on a targeted serum-based panel; thus, tissue-specific differences or proteins not captured in the current assay might still exist. Within the physiological systems surveyed by our targeted panels, 69 proteins exhibited differential expression in the patient group. Functional enrichment analyses revealed that many DEPs were significantly associated with regulating pathophysiological immune cell functions and inflammatory responses. These comprise altered inflammatory and defense responses, immune cell stimulation, interactions between cytokine families, recruitment of cell surface receptors in immune cells, activation of key intracellular signaling pathways, and the mediators of inflammatory cascades. Collectively, these findings provide robust evidence of a dysregulated inflammatory state in hEDS/HSD patients, aligning with the recent proteomic observations in an hEDS-specific cohort [22] and further supporting the evolving view that hEDS and HSD should not be considered exclusively connective tissue disorders [11, 38, 39]. Numerous extra-articular symptoms, extending beyond joint hypermobility, are frequently observed in patients with hEDS and HSD. These include a range of comorbidities such as mucocutaneous, osteoarticular, orthopedic, cardiovascular, muscular, gastrointestinal, neuropsychiatric, and atopic features, along with rheumatological manifestations such arthralgia, myalgia, and soft tissue injuries. In fact, multiple studies have documented an increased prevalence of immune-mediated disorders like rhinitis, asthma, urticaria, celiac disease, and neuropathies among these patients [7, 40–42]. Therefore, it is difficult to explain the

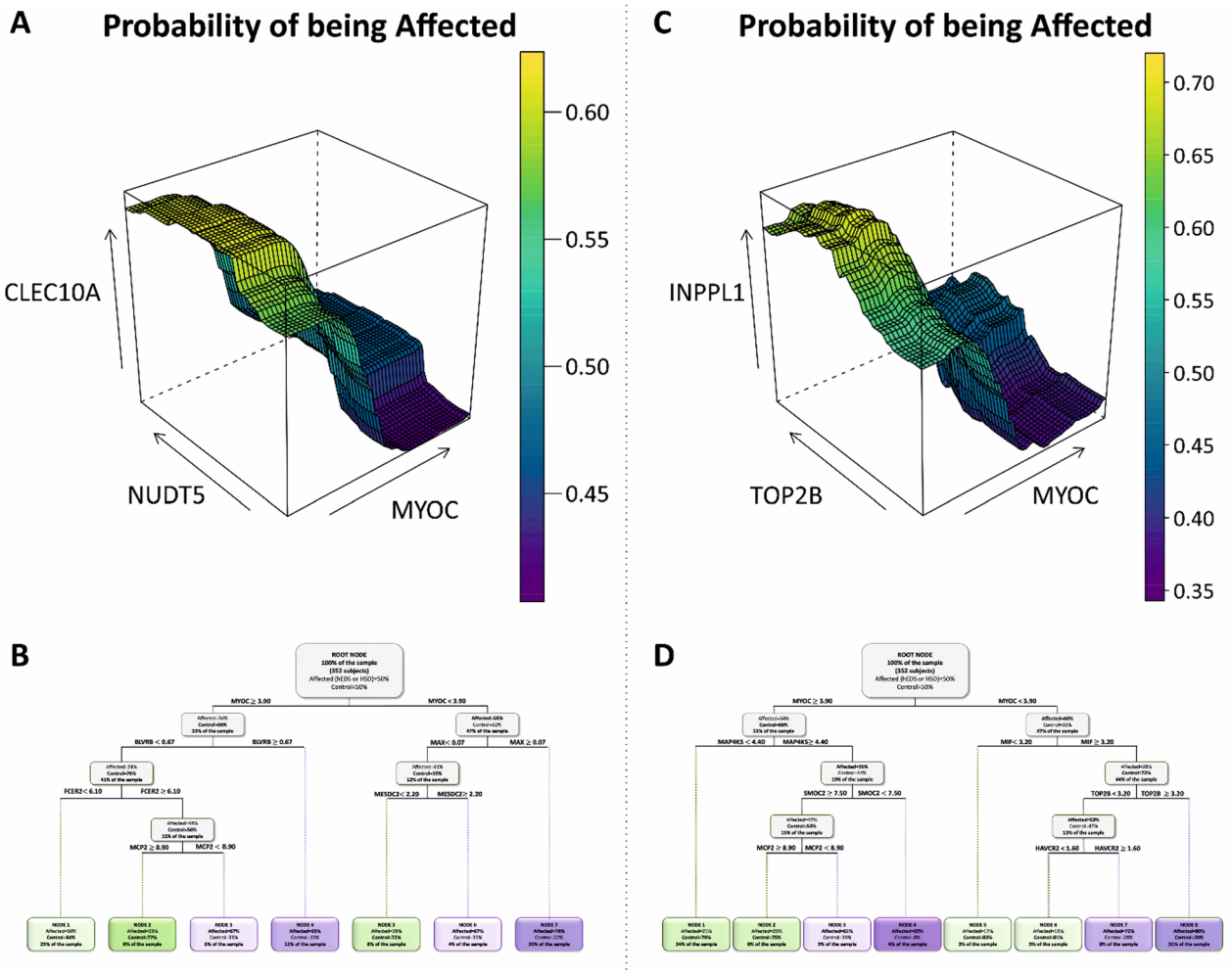

Fig. 4 3D-PDP and Classification tree. **A-C** (3D-PDP): the three-dimensional partial dependence plots illustrate how the probability of being classified as Affected (hEDS/HSD) changes according to the values of the three most important proteins selected by the RF with the relVIM. The color scale ranges from blue (lower probability) to yellow (higher probability), as shown by the side legends. Arrows on the x, y, and z-axes indicate the direction of increasing protein values. **A)** the probability of being classified as Affected reaches a maximum of 0.60, as shown by the yellow peak, when subjects show low values in correspondence of MYOC and high values for CLEC10A. (the role of NUDT5 is not determinant because the shape of the area tends to rise for median and high values). **C)** the probability of being classified as Affected reaches a maximum of 0.70 when subjects show low values of MYOC and high values of TOP2B and INPPL1. **B-D**: The classification trees group subjects into clusters according to their diagnosis (Affected vs. Control). At the top of the dendrogram (ROOT NODE) are all the individuals. At each step, the algorithm divides participants into two subgroups using a splitting criterion that selects the best proteins and corresponding cut-off values. Above each split (horizontal segment), the selected variable and corresponding rules of thumb are given. Grey rectangles represent intermediate clusters, reporting the percentage of Affected and Control subjects, with the predominant diagnosis highlighted in bold. Tree growth was limited by a pruning procedure, which defined the optimal structure with 7 final nodes in Figure B and 8 in Figure D. At the bottom, the terminal nodes (colored boxes) are labeled by the predominant diagnosis (purple = Affected, green = Control), with dashed lines connecting parent and final nodes. The most important variables appear in the top levels of the tree

broad spectrum of systemic manifestations as exclusively resulting from weakened connective tissue.

The complex involvement of multiple organ systems raises the question of a potential link between hEDS/HSD and rheumatologic disorders like rheumatoid arthritis (RA) and systemic lupus erythematosus (SLE) [43, 44]. Persistent low-grade inflammation may represent a plausible explanation for the observed overlap between hEDS/HSD and rheumatic diseases, potentially contributing to the disruption of connective tissue stability and joint pain. In this context, multiple studies have suggested that aberrant mast cell activation and the subsequent release of inflammatory mediators could compromise the integrity of connective tissue across multiple organ systems, potentially playing a role in the disease mechanisms within the hEDS/HSD spectrum. While specific studies on mast cell abnormalities in hEDS/HSD patients are still lacking, our present results, together with the overlap between mast cell-related diseases, immune-mediated disorders, and rheumatologic conditions affecting individuals with hEDS/HSD, point to a possible link among these disorders, characterized by

connective tissue abnormalities and inflammatory joint involvement [13, 44–48].

The present proteomic data point toward the possibility that hEDS and HSD may be compatible with different manifestations within a shared phenotypic spectrum, based on the presence of overlapping biological features observed in our dataset. This observation is consistent with our prior in vitro observations, in which hEDS and HSD fibroblasts exhibited a shared pro-inflammatory, matrix-degrading phenotype together with overlapping perturbations in gene expression [8, 9, 11, 21, 37]. Within our hypothesized disease framework, such a signaling environment might contribute to a self-reinforcing cycle in which aberrant ECM remodeling and persistent inflammatory signaling coexists, potentially impacting connective tissues integrity [11]. In parallel, and based on independent evidence, we have previously reported that ECM disorganization observed in patient-derived fibroblasts is associated with the observation of a specific circulating pattern of fibronectin and type I collagen fragments in the plasma of both hEDS and HSD patients [10] As these findings derive from distinct cohorts and experimental systems, no direct causal relationship can be inferred. Nevertheless, it is tempting to speculate that such ECM-derived fragments could act as damage-associated molecular patterns (DAMPs), thereby providing a hypothetical mechanistic link capable of contributing to the systemic inflammatory signatures identified in our proteomic analyses. This proposed cycle could be further sustained by immune and inflammatory mediators enriched in patient serum. Among these, the pleiotropic inflammatory cytokine macrophage migration inhibitory factor (MIF), which emerged as the most highly upregulated protein in our dataset. MIF appears to be a relevant therapeutic target in chronic inflammatory joint and arthritic diseases, including RA and SLE, as it is known to contribute to synovial and cartilage destruction and inflammatory processes implicated in the pathogenesis of such disorders [49]. Both research in mice and human clinical studies demonstrated the therapeutic potential of inhibiting MIF for treating RA and other chronic inflammatory diseases [49–51]. Another noteworthy protein is B cell scaffold protein with ankyrin repeats (BANK1) primarily expressed in B cells, which may be involved in the production of autoantibodies in SLE patients [52]. CD69 antigen, expressed by various immune and inflammatory cells (i.e., B and T lymphocytes, NK cells, monocytes, macrophages, neutrophils, and eosinophils), serves as an early leukocyte activation marker following various stimuli [53]. Its well-established pro-inflammatory effect has been observed in various autoimmune and chronic inflammatory disorders such as RA, SLE, and OA [54, 55]. Among the upregulated proteins, three members of the carbonic anhydrase (CA) family (CA1, CA2, and CA3) may also contribute to this pro-inflammatory state. CAs are metalloenzymes that catalyze the reversible hydration of carbon dioxide to bicarbonate [56]. Preclinical studies indicate that CAs play a substantial role in a wide range of pathological conditions, including neuropathic pain, chronic inflammatory joint and autoimmune conditions such as RA, SLE, and ankylosing spondylitis (AS) [56–58]. For example, transgenic mice that overexpress CA1, which recapitulate key features of RA and AS, exhibited increased joint inflammation, bone destruction, and tissue damage [59]. Consequently, developing selective inhibitors that target CAs continues to be explored as a potential approach for addressing these inflammatory and pain-related conditions [56, 60–62]. Overall, our results converge with these findings and further support the involvement of immune dysregulation and persistent inflammation in the pathogenesis of hEDS/HSD. The elevated serum expression of these proteins not only highlights their potential as candidate protein signatures but also opens avenues for developing targeted therapies aimed at alleviating musculoskeletal and chronic pain symptoms in affected individuals.

Beyond inflammation, our screening revealed abnormal serum levels of SIRT2, NTRK2, MYOC, and SOD1, proteins involved in Schwann cell development, differentiation, and myelin sheath formation [63]. Sirtuin 2 (SIRT2) modulates peripheral myelination by regulating cell polarity signaling pathways [64], while neurotrophic receptor tyrosine kinase 2 (NTRK2) plays a key role in neuronal development and survival, acting as a receptor for brain-derived neurotrophic factor [65]. Myocilin (MYOC) is a secreted glycoprotein expressed in Schwann cells that mediates myelination in the peripheral nervous system [66]. Schwann cells are glial cells essential for myelin production, enabling rapid impulses transmission and playing a critical role in nerve regeneration following injury [67]. This cell type has also been implicated in neuroinflammatory responses by recruiting macrophages to degrade myelin debris and activating the innate immune response via cytokines [68, 69]. While their role in neuropathic pain remains under investigation, they are recognized as potentially pro-nociceptive, particularly in inflammatory neuropathies and pain hyperalgesia [70, 71]. In this regard, it is noteworthy that neuropathic pain and small fiber neuropathy (SFN) are commonly reported comorbidities among hEDS/HSD patients [41, 72–75]. While the present proteomic findings do not provide direct evidence of nerve fiber damage, they underscore the potential involvement of the peripheral nervous system's regulatory environment. Chronic inflammation may expose Schwann cells to damaging oxidative stress over long periods, exacerbating cellular dysfunction and contributing to impaired connective tissue integrity. From a clinical perspective, exploring myelin-associated

mechanisms and their relationship to SFN may facilitate improved recognition of the complex hEDS/HSD pathology and help better stratify the heterogeneous patient population.

To prioritize promising candidates for future validation, we applied a multi-step machine learning approach. We first performed an RF analysis on the 69 proteins found differentially expressed between hEDS/HSD patients and controls. This approach allowed us to evaluate the relative contribution of each protein through the relVIM, as well as to explore their interactions using a 3D-PDP and a classification tree. Among the 69 proteins, MYOC, NUDT5, and CLEC10A emerged as the most informative in classifying affected individuals. Following this exploratory analysis, we applied the LASSO feature selection algorithm to the same set of DEPs to identify the optimal combination of candidate proteins. This predictive model selected 17 DEPs capable of separating cases from controls: CLEC10A, FCER2, HAVCR2, IL7, INPPL1, LXN, MAGED1, MAP4K5, MCP2, MIF, MYOC, NFC2, sFRP3, SMOC2, STXBP3, TNNI3, and TOP2B. Among them, the three most informative features according to relVIM were MYOC, TOP2B, and INPPL1. As previously described, MYOC is essential for peripheral nervous system myelination [66]. TOP2B (Topoisomerase II beta) is a nuclear enzyme that regulates DNA topology during transcription, playing a key role in gene expression in non-dividing cells such as neurons and contributing to neurodevelopmental and synaptic functions. INPPL1 (SHIP2) is a key regulator of the PI3K/AKT pathway through its phosphatidylinositol phosphatase activity and plays a multifaceted role in the ECM, including invadopodia formation, cell adhesion, and lymphatic vessel function. While these findings provide a prioritized foundation for future research aimed at developing objective laboratory-based tools for hEDS/HSD, we emphasize that these proteins represent a computationally derived discovery-phase signature rather than proven clinical biomarkers, and their translation requires several further limitations to be addressed. First, our findings are predicated on a targeted Proximity Extension Assay using five manufacturer-validated Olink® Target 96 panels: Neurology, Organ Damage, Development, Cardiometabolic, and Inflammation. While this platform offers an exceptional dynamic range and superior sensitivity for low-abundance biomarkers, it is restricted to a predefined set of 460 assays (458 unique proteins). Consequently, the proteomic landscape described here represents a targeted snapshot; significant biological signals residing outside these specific panels, including potential drivers in connective tissue remodeling or specialized metabolic signaling, remain uncaptured. Second, because these Olink panels are strategically curated for proteins with established pathological relevance, the identification of 69 DEPs should be interpreted as a result of targeted biological enrichment rather than a global, unbiased proteomic shift. This distinction is vital, as the density of our findings is naturally influenced by the assay's inherent focus on inflammatory, neurological, cardiometabolic, developmental, and organ-damage-related pathways. Third, to ensure the statistical stringency and power necessary to identify a robust, cross-population molecular signature, we chose to aggregate the Italian and American cohorts. While this approach effectively accounts for the high clinical heterogeneity of hEDS/HSD, we acknowledge the methodological trade-off of forgoing a traditional discovery-versus-validation split within the current study. Furthermore, as this was a cross-sectional analysis, the identified protein fluctuations represent a single physiological time point. This design does not account for the temporal dynamics of the disease or the influence of fluctuating comorbidities on the circulating proteome. Finally, the absence of orthogonal validation via secondary techniques such as ELISA, Western blotting, or mass spectrometry means these 69 DEPs should be considered discovery-phase candidates. While our application of stringent FDR-adjusted p-values significantly minimizes the risk of false positives, platform-specific artifacts cannot be entirely ruled out. These results provide a critical foundation for future research, which must employ independent cohorts and complementary technologies to confirm the mechanistic roles and eventual clinical utility of these circulating proteins.

Conclusions

In conclusion, the present targeted-serum proteomic analysis revealed a significant and shared dysregulation of circulating protein levels in both hEDS and HSD cohorts, providing a novel molecular perspective on the systemic nature of these disorders. While the precise mechanistic relationship of many of these proteins to hEDS/HSD pathophysiology remains to be fully elucidated, our results offer significant new insights into the underlying disease processes. In particular, the observed patterns are compatible with the involvement of chronic inflammatory signaling, imbalanced ECM turnover, and altered neuronal regulatory environments, thereby extending the traditional view of hEDS and HSD as conditions confined to isolated connective tissue defects. These findings should also be interpreted within the broader and evolving context of how hEDS and HSD are currently conceptualized in both clinical practice and research. The existing international diagnostic frameworks, including the 2017 classification, are largely based on expert consensus rather than objective molecular or laboratory-based markers, particularly for hEDS and HSD. This limitation has been widely acknowledged by the international EDS community and has motivated

coordinated efforts to refine disease classification and diagnostic criteria. Notably, initiatives such as the "Road to 2026," led by the International Consortium on EDS and Related Disorders in collaboration with The Ehlers-Danlos Society, aim to reassess and update current criteria to improve diagnostic precision, clinical utility, and global care pathways. Within this context, the identification of overlapping circulating protein signatures in hEDS and HSD is compatible with the growing recognition that these conditions may exist along a shared phenotypic and biological continuum rather than as fully distinct pathological entities. Ultimately, recognizing this shared systemic pathology represents an important step toward the development of supportive laboratory-based tools and targeted multi-modal therapeutic strategies, providing a framework for personalized care and improved clinical outcomes for this complex and underserved patient population.

Abbreviations

hEDS	Hypermobile Ehlers-Danlos syndrome
HCTD	Heritable connective tissue disorder
JHM	Joint hypermobility
HSD	Hypermobility spectrum disorders
ECM	Extracellular matrix
CM	Conditioned media
COLLI	Type I collagen
FN	Fibronectin
TNs	Tenascins
fs	Fragments
MMPs	Matrix metalloproteinases
DAMPs	Damage-associated molecular pattern
PEA	Proximity extension assay
5PQ	5-point questionnaire
MCAS	Mast cell activation syndrome
NPX	Normalized protein expression
QC	Quality control
DE	Differential expression
LOD	Limit of detection
N-Miss	Number of missing values
SD	Standard deviation
Q1	First quartile
Q3	Third quartile
BH	Benjamini-Hochberg
FDR	False discovery rate
LASSO	Least Absolute Shrinkage and Selection Operator
MSE	Mean Squared Error
RF	Random Forest
relVIM	Relative Variable Importance Measure
PDP	Partial Dependence Plot
DEPs	Differentially expressed proteins
GO	Gene Ontology (GO)
KEGG	Kyoto Encyclopedia of Genes and Genomes
POTS	Postural Orthostatic Tachycardia Syndrome
gHSD	Generalized HSD
BS	Beighton Score
BP	Biological process
MF	Molecular function
CC	Cellular component
RA	Rheumatoid arthritis
SLE	Systemic Lupus Erythematosus
MIF	Macrophage migration inhibitory factor
BANK1	B cell scaffold protein with ankyrin repeats
AS	Ankylosing spondylitis
SIRT2	Sirtuin 2
NTRK2	Neurotrophic receptor tyrosine kinase 2
MYOC	Myocilin
SFN	Small fiber neuropathy
DCs	Dendritic Cells
APC	Antigen presenting cells
SHIP2	Src Homology 2 Domain-containing Inositol Phosphatase 2

Supplementary Information

The online version contains supplementary material available at https://doi.org/10.1186/s12014-026-09588-2.

Supplementary Material 1

Supplementary Material 2

Supplementary Material 3

Supplementary Material 4

Supplementary Material 5

Supplementary Material 6

Supplementary Material 7

Supplementary Material 8

Supplementary Material 9

Supplementary Material 10

Supplementary Material 11

Supplementary Material 12

Supplementary Material 13

Supplementary Material 14

Acknowledgements

All authors express their sincere gratitude to the patients and their families, as well as healthy donors, for their kind availability for this study. Marco Ritelli, Nicola Chiarelli, Valeria Cinquina, Valeria Bertini, and Marina Colombi extend sincere thanks the Fazzo Cusan family for its generous support and to Ms. Jelena Skripac for her skilled technical assistance.

Author contributions

All authors have contributed to this article significantly. Conceptualization: M.R., V.C., N.C. and M.C.; formal analysis: M.R., V.C. and N.C.; investigation: V.C., N.C., V.B., G.C. and M.V.; resources: W.G., M.V. and M.R.; data curation: M.R., N.C., V.R., G.C., M.V. and M.C.; writing-original draft preparation, M.R., V.C., N.C. and M.C.; writing-review and editing: W.G.; visualization: M.R. and V.C.; supervision: M.R. and M.C.; funding acquisition: W.G. and M.R.; project administration: M.R. All authors have read and agreed to the published version of the manuscript.

Funding

This research was funded by The Ehlers-Danlos Society to MR within the "Molecular Studies in hEDS and HSD Grants: Targeted serum proteomics through proximity extension assay to unravel biomarkers for hypermobile Ehlers-Danlos syndrome and hypermobility spectrum disorders".

Data availability

Most data generated or analyzed during this study are included in this published article and its Additional files. Additional data and materials are available from the corresponding author on reasonable request, subject to compliance with our obligations under human research ethics.

Declarations

Ethics approval and consent to participate

The study was approved by the local Ethical Committee "Comitato Etico di Brescia, ASST degli Spedali Civili, Brescia" in Italy (Protocol numbers NP5582) and by the "Genetic Alliance Institutional Review Board" in the USA (Federal Registration Number IORG0003358, Project number EDS002).

Patient consent statement
All subjects provided written informed consent for their inclusion in the study and for the use of their clinical data and samples for research purposes.

Competing interests
The authors declare no competing interests.

Author details
[1]Department of Molecular and Translational Medicine, Università degli Studi di Brescia, Brescia, Italy
[2]Department of Clinical and Experimental Science, Università degli Studi di Brescia and Division of Dermatology, ASST Spedali Civili di Brescia, Brescia, Italy
[3]The Ehlers-Danlos Society, New York, NY, USA

Received: 26 September 2025 / Accepted: 2 February 2026
Published online: 07 March 2026

References

1. Tinkle B, Castori M, Berglund B, Cohen H, Grahame R, Kazkaz H et al. Hypermobile Ehlers–Danlos syndrome (a.k.a. Ehlers–Danlos syndrome Type III and Ehlers–Danlos syndrome hypermobility type): Clinical description and natural history. Am J Med Genet C Semin Med Genet. 2017r;175(1):48-69. https://doi.org/10.1002/ajmg.c.31538
2. Malfait F, Francomano C, Byers P, Belmont J, Berglund B, Black J, et al. The 2017 international classification of the Ehlers–Danlos syndromes.Am J Med Genet C Semin Med Genet. 2017;175(1):8-26. http://doi.org/10.1002/ajmg.c.31552.
3. Malfait F, Castori M, Francomano CA, Giunta C, Kosho T, Byers PH. The Ehlers–Danlos syndromes.Nat Rev Dis Primers. 2020;6(1):64. https://doi.org/10.1038/s41572-020-0194-9
4. Castori M, Tinkle B, Levy H, Grahame R, Malfait F, Hakim A. A framework for the classification of joint hypermobility and related conditions. Am J Med Genet C Semin Med Genet. 2017;175(1):148-157. https://doi.org/10.1002/ajmg.c.31539
5. Gensemer C, Burks R, Kautz S, Judge DP, Lavallee M, Norris RA. Hypermobile Ehlers-Danlos syndromes: Complex phenotypes, challenging diagnoses, and poorly understood causes. Dev Dyn. 2021 ;250(3):318-344. https://doi.org/10.1002/dvdy.220
6. Carroll MB. Hypermobility spectrum disorders: A review.]Rheumatol Immunol Res. 2023;22;4(2):60-68. https://doi.org/10.2478/rir-2023-0010
7. Ritelli M, Chiarelli N, Cinquina V, Vezzoli M, Venturini M, Colombi M. Looking back and beyond the 2017 diagnostic criteria for hypermobile Ehlers-Danlos syndrome: A retrospective cross-sectional study from an Italian reference centerAm J Med Genet A. 2024;194(2):174-194. https://doi.org/10.1002/ajmg.a.63426
8. Chiarelli N, Zoppi N, Ritelli M, Venturini M, Capitanio D, Gelfi C et al. Biological insights in the pathogenesis of hypermobile Ehlers-Danlos syndrome from proteome profiling of patients' dermal myofibroblasts. Biochim Biophys Acta Mol Basis Dis. 2021;1867(4):166051. https://doi.org/10.1016/j.bbadis.2020.166051
9. Chiarelli N, Zoppi N, Venturini M, Capitanio D, Gelfi C, Ritelli M et al. Matrix metalloproteinases inhibition by doxycycline rescues extracellular matrix organization and partly reverts myofibroblast differentiation in hypermobile ehlers-danlos syndrome dermal fibroblasts: A potential therapeutic target? Cells. 2021;10(11):3236. https://doi.org/10.3390/cells10113236
10. Ritelli M, Chiarelli N, Cinquina V, Bertini V, Piantoni S, Caproli A, et al. Bridging the diagnostic gap for Hypermobile Ehlers-Danlos Syndrome and Hypermobility Spectrum Disorders: evidence of a common extracellular matrix fragmentation pattern in patient plasma as a potential biomarker. Am J Med Genet A. 2025. https://doi.org/10.1002/ajmg.a.63857.
11. Ritelli M, Chiarelli N, Cinquina V, Zoppi N, Bertini V, Venturini M et al. RNA-Seq of Dermal Fibroblasts from Patients with Hypermobile Ehlers–Danlos Syndrome and Hypermobility Spectrum Disorders Supports Their Categorization as a Single Entity with Involvement of Extracellular Matrix Degrading and Proinflammatory Pathomechanism. Cells2022;11(24):4040. https://doi.org/10.3390/cells11244040
12. Demmler JC, Atkinson MD, Reinhold EJ, Choy E, Lyons RA, Brophy ST. Diagnosed prevalence of Ehlers-Danlos syndrome and hypermobility spectrum disorder in Wales, UK: a national electronic cohort study and case-control comparison. BMJ Open. 2019;9(11):e031365. https://doi.org/10.1136/bmjopen-2019-031365
13. Hakim AJ, Tinkle BT, Francomano CA. Ehlers–Danlos syndromes, hypermobility spectrum disorders, and associated co-morbidities: Reports from EDS ECHO. Am J Med Genet C Semin Med Genet. 2021;187(4):413-415. https://doi.org/10.1002/ajmg.c.31954
14. Halverson CME, Clayton EW, Garcia Sierra A, Francomano C. Patients with Ehlers–Danlos syndrome on the diagnostic odyssey: rethinking complexity and difficulty as a hero's journey. Am J Med Genet C Semin Med Genet. 2021;187:416–24. http://doi.orh/10.1002/ajmg.c.31935.
15. Daylor V, Griggs M, Weintraub A, Byrd R, Petrucci T, Huff M et al. Defining the Clinical Complexity of hEDS and HSD: A Global Survey of Diagnostic Challenge, Comorbidities, and Unmet Needs.J Clin Med. 2025;14(16):5636. https://doi.org/10.3390/jcm14165636
16. Wang YT, Jahani S, Morel-Swols D, Kapely A, Rosen A, Forghani I. Patient experiences of receiving a diagnosis of hypermobile Ehlers–Danlos syndrome. Am J Med Genet Part A. 2024;194(8):e63613. https://doi.org/10.1002/ajmg.a.63613
17. Lee C, Chopra P. The incidence of misdiagnosis in patients with Ehlers–Danlos syndrome. Children (Basel). 2025;12:698. https://doi.org/10.3390/children12060698.
18. Anderson LK, Lane KR. The diagnostic journey in adults with hypermobile Ehlers-Danlos syndrome and hypermobility spectrum disorders. J Am Assoc Nurse Pract. 2022. https://doi.org/10.1097/JXX.0000000000000672.
19. Black WR, Black LL, Goldstein-Leever A, Fox LS, Pratt LR, Jones JT. The need for primary care providers in the clinical management of hypermobility spectrum disorders and ehlers-danlos syndrome: a call to action. Rheumatol Int. 2024;44:2273–8. https://doi.org/10.1007/s00296-024-05676-4
20. Atwell K, Michael W, Dubey J, James S, Martonffy A, Anderson S, et al. Diagnosis and management of hypermobility spectrum disorders in primary care. J Am Board Fam Med. 2021. https://doi.org/10.3122/jabfm.2021.04.200374.
21. Zoppi N, Chiarelli N, Binetti S, Ritelli M, Colombi M. Dermal fibroblast-to-myofibroblast transition sustained by αvß3 integrin-ILK-Snail1/Slug signaling is a common feature for hypermobile Ehlers-Danlos syndrome and hypermobility spectrum disorders. Biochim Biophys Acta Mol Basis Dis. 2018;1864(4 Pt A):1010-1023. https://doi.org/10.1016/j.bbadis.2018.01.005
22. Griggs M, Daylor V, Petrucci T, Weintraub A, Huff M, Willey S, et al. Proteomic discoveries in hypermobile Ehlers–Danlos syndrome reveal insights into disease pathophysiology. ImmunoHorizons. 2025. https://doi.org/10.1093/immhor/vlaf044.
23. Watanabe A, Satoh K, Maniwa T, Matsumoto KI. Proteomic analysis for the identification of serum diagnostic markers for joint hypermobility syndrome. Int J Mol Med. 2016;37(2):461-7. https://doi.org/10.3892/ijmm.2015.2437
24. Lundberg M, Eriksson A, Tran B, Assarsson E, Fredriksson S. Homogeneous antibody-based proximity extension assays provide sensitive and specific detection of low-abundant proteins in human blood. Nucleic Acids Res. 2011;39:e102. https://doi.org/10.1093/nar/gkr424.
25. Hakim AJ, Grahame R. A simple questionnaire to detect hypermobility: An adjunct to the assessment of patients with diffuse musculoskeletal pain. Int J Clin Pract. 2003;57(3):163-6 https://doi.org/10.1111/j.1742-1241.2003.tb10455.x
26. Tibshirani R. Regression shrinkage and selection via the Lasso. J R Stat Soc Ser B Methodol. 1996;58:267–88.https://doi.org/10.1111/j.1467-9868.2011.00771.x
27. Stekhoven DJ, Bühlmann P. Missforest-Non-parametric missing value imputation for mixed-type data. Bioinformatics. 2012;28(1):112-8. https://doi.org/10.1093/bioinformatics/btr597
28. Vezzoli M, Inciardi RM, Oriecuia C, Paris S, Murillo NH, Agostoni P et al. Machine learning for prediction of in-hospital mortality in coronavirus disease 2019 patients: Results from an Italian multicenter study. J Cardiovasc Med (Hagerstown). 2022;23(7):439-446. https://doi.org/10.2459/JCM.0000000000001329
29. Breiman, L. Random Forests. Machine Learning. 2001;45:5–32. https://doi.org/10.1023/A:1010933404324
30. Micheletti S, Galli J, Vezzoli M, Scaglioni V, Agostini S, Calza S et al. Academic skills in children with cerebral palsy and specific learning disorders. Dev Med Child Neurol. 2024;66(6):778-792. https://doi.org/10.1111/dmcn.15808
31. Doglietto F, Vezzoli M, Gheza F, Lussardi GL, Domenicucci M, Vecchiarelli L et al. Factors Associated with Surgical Mortality and Complications among Patients with and without Coronavirus Disease 2019 (COVID-19) in Italy. JAMA Surg. 2020;155(8):691-702. https://doi.org/10.1001/jamasurg.2020.2713

32. Vezzoli M. Exploring the facets of overall job satisfaction through a novel ensemble learning. Electron J Appld Statl Anal. 2011;4:23-38. https://doi.org/10.1285/I20705948V4N1P23
33. Carpita M, Vezzoli M. Statistical evidence of the subjective work quality: the fairness drivers of the job satisfaction. Electron J Appl Stat Anal. 2012;5:89–107. https://doi.org/10.1285/i20705948v5n1p89
34. Garrafa E, Segala A, Vezzoli M, Bottani E, Zanini B, Vetturi A et al. Mitochondrial Dysfunction in Peripheral Blood Mononuclear Cells as Novel Diagnostic Tools for Non-Alcoholic Fatty Liver Disease: Visualizing Relationships with Known and Potential Disease Biomarkers. Diagnostics (Basel). 2023;13(14):2363. https://doi.org/10.3390/diagnostics13142363
35. Friedman JH. Greedy function approximation: a gradient boosting machine. Ann Stat. 2001;29:1189–232. https://doi.org/10.1214/aos/1013203451
36. Wu T, Hu E, Xu S, Chen M, Guo P, Dai Z, et al. clusterProfiler 4.0: a universal enrichment tool for interpreting omics data. Innovation (Camb). 2021;2:100141. https://doi.org/10.1016/j.xinn.2021.100141.
37. Chiarelli N, Carini G, Zoppi N, Dordoni C, Ritelli M, Venturini M, et al. Transcriptome-wide expression profiling in skin fibroblasts of patients with joint hypermobility syndrome/ehlers-danlos syndrome hypermobility type. PLoS One. 2016. https://doi.org/10.1371/journal.pone.0161347.
38. Martin A. An acquired or heritable connective tissue disorder? A review of hypermobile Ehlers Danlos Syndrome. Eur J Med Genet. 2019;62(7):103672. https://doi.org/10.1016/j.ejmg.2019.103672
39. Alsiri N, Alhadhoud M, Alkatefi T, Palmer S. The concomitant diagnosis of fibromyalgia and connective tissue disorders: A systematic review.emin Arthritis Rheum. 2023;58:152127 https://doi.org/10.1016/j.semarthrit.2022.152127
40. Wasim S, Suddaby JS, Parikh M, Leylachian S, Ho B, Guerin A et al. Pain and gastrointestinal dysfunction are significant associations with psychiatric disorders in patients with Ehlers-Danlos syndrome and hypermobility spectrum disorders: a retrospective study. Rheumatol Int. 2019;39(7):1241-1248. https://doi.org/10.1007/s00296-019-04293-w
41. Fernandez A, Aubry-Rozier B, Vautey M, Berna C, Suter MR. Small fiber neuropathy in hypermobile Ehlers Danlos syndrome/hypermobility spectrum disorder. J Intern Med. 2022;292(6):957-960. https://doi.org/10.1111/joim.13539
42. Aubry-Rozier B, Schwitzguebel A, Valerio F, Tanniger J, Paquier C, Berna C et al. Are patients with hypermobile Ehlers–Danlos syndrome or hypermobility spectrum disorder so different? Rheumatol Int. 2021;41(10):1785-1794 https://doi.org/10.1007/s00296-021-04968-3
43. Rodgers KR, Gui J, Dinulos MBP, Chou RC. Ehlers-Danlos syndrome hypermobility type is associated with rheumatic diseases.Sci Rep. 2017;7:39636. https://doi.org/10.1038/srep39636
44. Monaco A, Choi D, Uzun S, Maitland A, Riley B. Association of mast-cell-related conditions with hypermobile syndromes: a review of the literature. Immunol Res. 2022;70(4):419-431. https://doi.org/10.1007/s12026-022-09280-1
45. Vazquez M, Chovanec J, Kim J, DiMaggio T, Milner JD, Francomano CA et al. Hereditary alpha-tryptasemia modifies clinical phenotypes among individuals with congenital hypermobility disorders. HGG Adv. 2022;3(2):100094. https://doi.org/10.1016/j.xhgg.2022.100094
46. Brock I, Prendergast W, Maitland A. Mast cell activation disease and immunoglobulin deficiency in patients with hypermobile Ehlers-Danlos syndrome/hypermobility spectrum disorder. Am J Med Genet C Semin Med Genet. 2021;187(4):473-481. https://doi.org/10.1002/ajmg.c.31940
47. Afrin LB. Some cases of hypermobile Ehlers–Danlos syndrome may be rooted in mast cell activation syndrome. Am J Med Genet C Semin Med Genet. 2021;187(4):466-472. https://doi.org/10.1002/ajmg.c.31944
48. Gutowski Ł, Kanikowski S, Formanowicz D. Mast Cell Involvement in the Pathogenesis of Selected Musculoskeletal Diseases. Life (Basel). 2023;13(8):1690. https://doi.org/10.3390/life13081690
49. Bilsborrow JB, Doherty E, Tilstam PV, Bucala R. Macrophage migration inhibitory factor (MIF) as a therapeutic target for rheumatoid arthritis and systemic lupus erythematosus. Expert Opin Ther Targets. 2019;23(9):733-744. https://doi.org/10.1080/14728222.2019.1656718
50. Grieb G, Merk M, Bernhagen J, Bucala R. Macrophage Migration Inhibitory Factor (MIF): A promising biomarker.Drug News Perspect. 2010;23(4):257-64. https://doi.org/10.1358/dnp.2010.23.4.1453629
51. Ferhat M, Mangano K, Mirkina I, Mayer J, Rossmueller G, Schinagl A et al. The newly engineered monoclonal antibody ON104, targeting the oxidized Macrophage Migration Inhibitory Factor (oxMIF), ameliorates clinical and histopathological signs of collagen-induced arthritis.Eur J Pharmacol. 2023;956:175997. https://doi.org/10.1016/j.ejphar.2023.175997
52. Satterthwaite AB. TLR7 Signaling in Lupus B Cells: New Insights into Synergizing Factors and Downstream Signals. Curr Rheumatol Rep. 2021;23(11):80. https://doi.org/10.1007/s11926-021-01047-1
53. Gorabi AM, Hajighasemi S, Kiaie N, Gheibi Hayat SM, Jamialahmadi T, Johnston TP, et al. The pivotal role of CD69 in autoimmunity. J Autoimmun. 2020;111:102453. https://doi.org/10.1016/j.jaut.2020.102453
54. González-Amaro R, Cortés JR, Sánchez-Madrid F, Martín P. Is CD69 an effective brake to control inflammatory diseases?Trends Mol Med. 2013;19(10):625-32. https://doi.org/10.1016/j.molmed.2013.07.006
55. Vitales-Noyola M, Oceguera-Maldonado B, Niño-Moreno P, Baltazar-Benítez N, Baranda L, Layseca-Espinosa E et al. Patients with Systemic Lupus Erythematosus Show Increased Levels and Defective Function of CD69 + T Regulatory Cells. Mediators Inflamm. 2017;2017:2513829. https://doi.org/10.1155/2017/2513829
56. Mishra CB, Tiwari M, Supuran CT. Progress in the development of human carbonic anhydrase inhibitors and their pharmacological applications: Where are we today? Med Res Rev. 2020;40(6):2485-2565. https://doi.org/10.1002/med.21713
57. Supuran CT. Carbonic anhydrase inhibition and the management of neuropathic pain. Expert Rev Neurother. 2016;16(8):961-8. https://doi.org/10.1080/14737175.2016.1193009
58. Micheli L, Bozdag M, Akgul O, Carta F, Guccione C, Bergonzi MC et al. Pain relieving effect of-NSAIDS-CAIs hybrid molecules: Systemic and intra-articular treatments against rheumatoid arthritis. Int J Mol Sci. 2019;20(8):1923. https://doi.org/10.3390/ijms20081923
59. Zheng Y, Wang L, Zhang W, Xu H, Chang X. Transgenic mice over-expressing carbonic anhydrase i showed aggravated joint inflammation and tissue destruction.Musculoskelet Disord. 2012;13:256. https://doi.org/10.1186/1471-2474-13-256
60. Bua S, Di Cesare Mannelli L, Vullo D, Ghelardini C, Bartolucci G, Scozzafava A et al. Design and Synthesis of Novel Nonsteroidal Anti-Inflammatory Drugs and Carbonic Anhydrase Inhibitors Hybrids (NSAIDs-CAIs) for the Treatment of Rheumatoid Arthritis.J Med Chem. 2017;60(3):1159-1170. https://doi.org/10.1021/acs.jmedchem.6b01607
61. Carta F, Di Cesare Mannelli L, Pinard M, Ghelardini C, Scozzafava A, McKenna R et al. A class of sulfonamide carbonic anhydrase inhibitors with neuropathic pain modulating effects. Bioorg Med Chem. 2015;23(8):1828-40. https://doi.org/10.1016/j.bmc.2015.02.027
62. Supuran CT. Drug interactions of carbonic anhydrase inhibitors and activators. Expert Opin Drug Metab Toxicol. 2024;20(3):143-155. https://doi.org/10.1080/17425255.2024.2328152
63. Dermitzakis I, Manthou ME, Meditskou S, Miliaras D, Kesidou E, Boziki M et al. Developmental Cues and Molecular Drivers in Myelinogenesis: Revisiting Early Life to Re-Evaluate the Integrity of CNS Myelin.Curr Issues Mol Biol. 2022;44(7):3208-3237. https://doi.org/10.3390/cimb44070222
64. Beirowski B, Gustin J, Armour SM, Yamamoto H, Viader A, North BJ et al. Sir-two-homolog 2 (Sirt2) modulates peripheral myelination through polarity protein Par-3/atypical protein kinase C (aPKC) signaling. Proc Natl Acad Sci U S A. 2011;108(43):E952-61. https://doi.org/10.1073/pnas.1104969108
65. Roussel-Gervais A, Sgroi S, Cambet Y, Lemeille S, Seredenina T, Krause KH et al. Genetic knockout of NTRK2 by CRISPR/Cas9 decreases neurogenesis and favors glial progenitors during differentiation of neural progenitor stem cells. Front Cell Neurosci. 2023;17:1289966. https://doi.org/10.3389/fncel.2023.1289966
66. Kwon HS, Johnson TV, Joe MK, Abu-Asab M, Zhang J, Chan CC, et al. Myocilin mediates myelination in the peripheral nervous system through ErbB2/3 signaling. J Biol Chem. 2013;288(37):26357-71. https://doi.org/10.1074/jbc.M112.446138
67. Balakrishnan A, Belfiore L, Chu TH, Fleming T, Midha R, Biernaskie J et al. Insights Into the Role and Potential of Schwann Cells for Peripheral Nerve Repair From Studies of Development and Injury. Front Mol Neurosci. 2021;13:608442. https://doi.org/10.3389/fnmol.2020.608442
68. Ydens E, Lornet G, Smits V, Goethals S, Timmerman V, Janssens S. The neuroinflammatory role of Schwann cells in disease. Neurobiol Dis. 2013;55:95–103. https://doi.org/10.1016/j.nbd.2013.03.005
69. Özdağ Acarlı AN, Klein T, Egenolf N, Sommer C, Üçeyler N. Subepidermal Schwann cell counts correlate with skin innervation – an exploratory study. Muscle Nerve. 2022;65:471–9. https://doi.org/10.1002/mus.27496

70. Wei Z, Fei Y, Su W, Chen G. Emerging role of schwann cells in neuropathic pain: receptors, glial mediators and myelination. Front Cell Neurosci. 2019;13:445946. https://doi.org/10.3389/fncel.2019.00116.
71. Wang Q, Chen FY, Ling ZM, Su WF, Zhao YY, Chen G, et al. The effect of Schwann cells/Schwann cell-like cells on cell therapy for peripheral neuropathy. Front Cell Neurosci. 2022;16:836931. 4https://doi.org/10.3389/fncel.2022.836931
72. Igharo D, Thiel JC, Rolke R, Akkaya M, Weis J, Katona I et al. Skin biopsy reveals generalized small fibre neuropathy in hypermobile Ehlers–Danlos syndromes. Eur J Neurol. 2023;30(3):719-728. https://doi.org/10.1111/ene.15649
73. Cazzato D, Castori M, Lombardi R, Caravello F, Bella ED, Petrucci A et al. Small fiber neuropathy is a common feature of Ehlers-Danlos syndromes. Neurology. 2016;87(2):155-9. https://doi.org/10.1212/WNL.0000000000002847
74. Leone CM, Celletti C, Gaudiano G, Puglisi PA, Fasolino A, Cruccu G et al. Pain due to ehlers-danlos syndrome is associated with deficit of the endogenous pain inhibitory control. Pain Med. 2020;21(9):1929-1935. https://doi.org/10.1093/pm/pnaa038
75. Pascarella A, Provitera V, Lullo F, Stancanelli A, Saltalamacchia AM, Caporaso G et al. Evidence of small fiber neuropathy in a patient with Ehlers–Danlos syndrome, hypermobility-type. Clin Neurophysiol. 2016;127(3):1914-6. https://doi.org/10.1016/j.clinph.2015.12.004

Publisher's note